NJC

ROYAL SOCIETY OF CHEMISTRY

PAPER

View Article Online
View Journal | View Issue

Cite this: *New J. Chem.*, 2025, **49**, 18282

Synthesis and physicochemical properties of (5-thiaporphyrinato)zinc and linear tetrapyrroles carrying a thioketo group

Hideki Uno, Muneki Hayakawa, Akuto Takagi and Tadashi Mizutani *

Received 3rd June 2025,
Accepted 2nd September 2025

DOI: 10.1039/d5nj02301g

rsc.li/njc

Sulfur analogues of bilin-1-one and bilin-1,19-dione were prepared and their spectroscopic properties and reactivities were investigated. *meso*-Arylbilin-1,19-dione, obtained by coupled oxidation of iron *meso*-arylporphyrin, was converted to 19-thioxobilin-1-one *via* the 5-oxaporphyrin zinc complex. The 5-thiaporphyrin zinc complex was prepared by cyclization of 19-thioxobilin-1-one in 78% yield at 0 °C. At higher temperatures a mixture of (5-thiaporphyrinato)zinc and (5-oxaporphyrinato)zinc was obtained. The temperature-dependent regioselectivity was ascribed to a lower activation energy of cyclization of bilin-1-thione than that of bilin-1-one. Ring-opening of (5-thiaporphyrinato)zinc with benzenethiolate gave 19-phenylsulfanylbilin-1-thione. The rate constant of formation of (5-thiaporphyrinato)zinc from 19-phenylsulfanylbilin-1-thione (0.01 mM) and zinc acetate (0.1 mM) in CH_3CN–H_2O (1/1) at 25 °C was 10^4 times larger than that of 19-phenylsulfanylbilin-1-one. Copper(II), cobalt(II), nickel(II), magnesium and cadmium ions also induced cyclization of 19-phenylsulfanylbilin-1-thione to afford the corresponding metal complexes of 5-thiaporphyrin. The sulfur analogues of bilin-1-one and bilin-1,19-dione showed bathochromically shifted UV-visible spectra, up to 100 nm, compared to the corresponding bilin-1-one and bilin-1,19-dione. Due to much higher reactivity and lower energy gap of bilin-1-thione than bilin-1-one, linear tetrapyrroles with a thioketo group should find applications in chemistry, biochemistry and materials science.

Introduction

Porphyrins and phthalocyanines are important tetrapyrrolic dyes and find applications in diverse fields such as biological and materials science. Carbon atoms bridge pyrroles in porphyrin while nitrogen atoms bridge pyrroles in porphyrazine and phthalocyanine. 5-Oxaporphyrin, in which an oxygen atom bridges pyrroles, has received attention, because an iron complex of 5-oxaporphyrin is an intermediate of catabolism of heme catalyzed by heme oxygenase.[1–3] Introduction of nitrogen or oxygen atoms into the aromatic framework of porphyrin lowers the energy levels of the frontier orbitals (Table S1), causing significant changes in the reactivity as well as their optical and redox properties. Preparation of *meso*-heteroatom porphyrins and related compounds has been the subject of studies in recent decades.[4,5] For instance, 5-oxaporphyrin has been used as a precursor for various linear tetrapyrroles,[6] that constitute an important class of dyes frequently employed in biological[7–9] and functional materials research.[10–13] Compared to 5-oxaporphyrin, fewer investigations were reported for 5-thiaporphyrin.[14–16]

Department of Applied Chemistry, Faculty of Science and Engineering, Doshisha University, 1-3, Tatara-miyakotani, Kyotanabe, Kyoto, 610-0394, Japan. E-mail: tmizutan@mail.doshisha.ac.jp

Since the electronegativity of sulfur is close to that of carbon, the electronic properties of 5-thiaporphyrin are expected to be similar to those of porphyrin. For chemical stability of these analogues, Fuhrhop *et al.* reported that ring-opening reactions of *meso*-heteroatom porphyrins proceed under basic and acidic conditions, with the relative stability decreasing in the order, 5-methine- > 5-aza- ≫ 5-thia- > 5-oxaporphyrins.[17] The previously reported 5-heteroporphyrins have been substituted with eight alkyl groups at the β-positions of the pyrrole rings. In contrast, we have reported the synthesis and reactivity of 5-oxaporphyrins bearing four phenyl groups at the *meso*-positions.[18] We conducted a kinetic study of the cyclization reaction of bilinthione leading to the formation of 5-thiaporphyrin, which has been scarcely reported in previous studies, in comparison with the cyclization reactions of its oxygen analogues. Linear tetrapyrroles having a thioketo group at the terminal such as 19-thioxobilin-1-one **3** showed much higher reactivity than the corresponding oxygen analogue, due to the higher nucleophilicity of sulfur. We showed that ring-closing reaction of bilin-1-thione proceeded 10^4 faster than its oxygen analogue. We focus on the reversible reactions of linear tetrapyrroles and *meso*-heteroatom porphyrins, where condensation–cyclization (CC) and nucleophilic ring-opening (NR) reactions are involved (see Scheme 1).

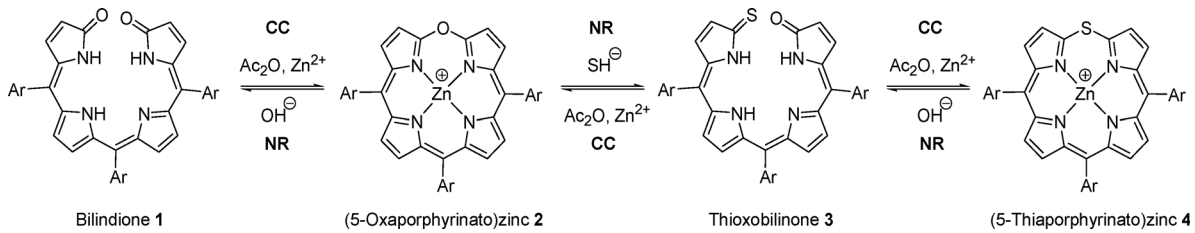

Scheme 1 Reversible nucleophilic ring-opening (NR) and condensation–cyclization (CC) reactions of bilindiones and 5-oxa- or 5-thiaporphyrins. Ar = p-C_6H_4–$COOCH_3$.

Results and discussion

Synthesis of (5-thiaporphyrinato)zinc

No studies have been reported on how the reactivity of linear tetrapyrroles bearing a thioketo group differs from that of their oxygen analogues. To address this question, we first carried out the synthesis of 5-thiaporphyrin, which is a key precursor for various linear tetrapyrroles having a thioketo group at the terminal. Preparation of (5-thiaporphyrinato)zinc is shown in Scheme 2. Bilindione **1** was prepared by coupled oxidation of iron tetraarylporphyrin **5**.[19–22] In this reaction, biladienone **6** was obtained as a major product,[23] and bilindione **1** was obtained as a minor one. Ring-closing reaction of bilindione **1** to (5-oxaporphyrinato)zinc **2** was performed according to the Fuhrhop procedure to quantitatively obtain the (5-oxaporphyrinato)zinc **2**. We also found that the acyl group of biladienone **6** was successfully cleaved to obtain the 5-oxaporphyrin copper complex **7** in the previous paper.[24] Because biladienones can be prepared from tetraarylporphyrin in various ways,[25–30] transformation of biladienone to 5-oxaporphyrin is synthetically useful and highly valuable. These 5-oxaporphyrins are versatile precursors for various bilinones, using nucleophilic ring-opening reactions shown in Scheme 1. The yield of

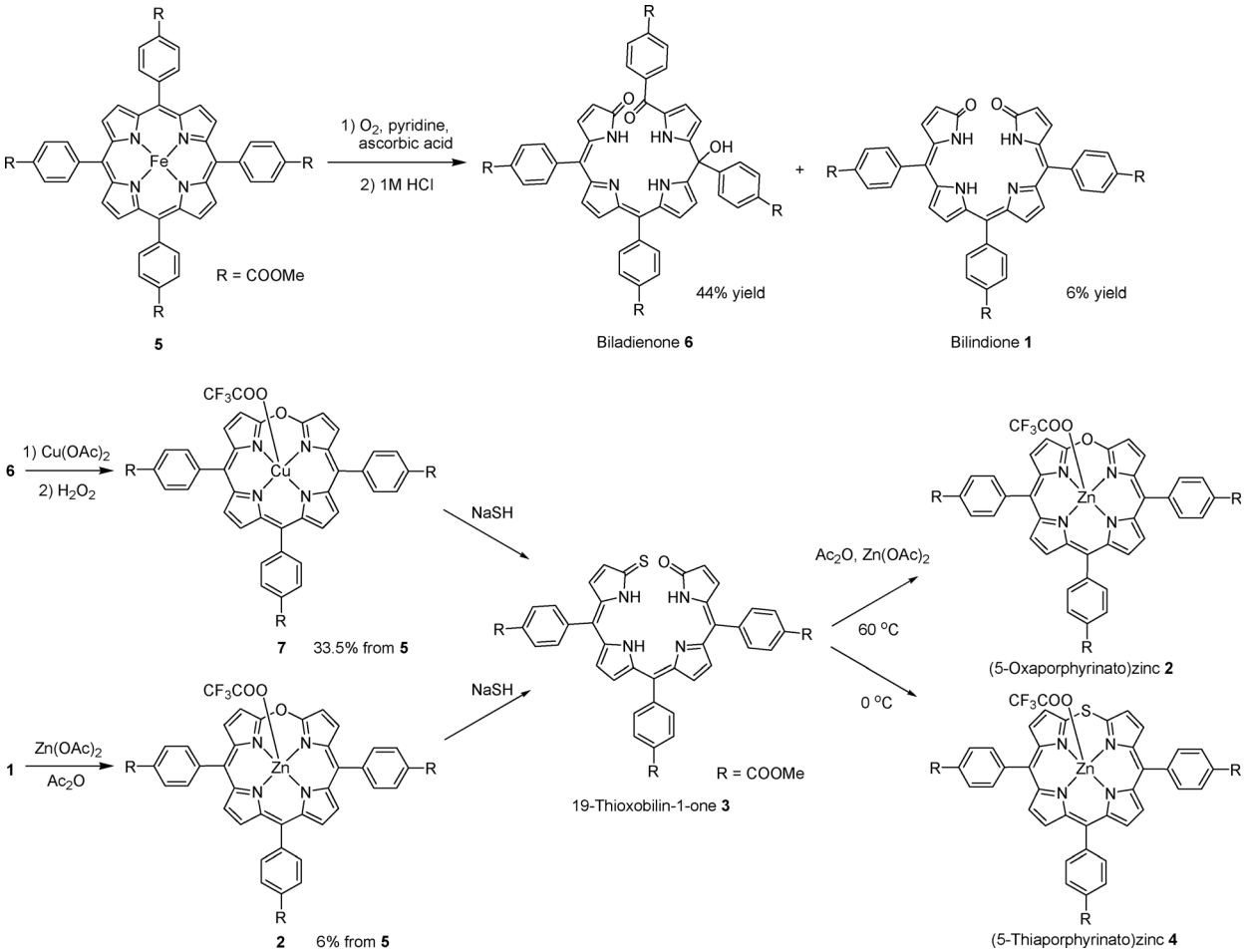

Scheme 2 Preparation of (5-thiaporphyrinato)zinc **4** from (tetraarylporphyrinato)iron(II) **5**. Compounds **2**, **4**, and **7** were isolated as CF_3COO^- salts using trifluoroacetic acid-containing eluant for column chromatography.

5-oxaporphyrins **7** and **2** from the iron porphyrin **5** was 33.5 and 6%, respectively. The reaction of **7** and **2** with NaSH proceeded quickly to yield 19-thioxobilin-1-one **3** (Scheme 2).[31] We attempted to prepare 5-thiaporphyrin by ring-closing reaction of 19-thioxobilinone **3**.

However, the reaction resulted in unexpected results. Fuhrhop *et al.*[32] and Saito *et al.*[33] reported the conversion of bilin-1,19-dione to (5-oxaporphyrinato)zinc by refluxing bilin-1,19-dione, zinc acetate, and acetic anhydride. Shinokubo and coworkers reported that cyclization of octaethyl-19-thioxo-1-bilinone with trifluoromethanesufonic anhydride at room temperature yielded 30% 5-thiaporphyrinium cation and 1% 5-oxaporphyrinium cation.[16] Reaction of 19-thioxobilin-1-one **3** with zinc acetate and acetic anhydride at room temperature for 30 min gave a 1 : 1 mixture of (5-oxaporphyrinato)zinc **2** and (5-thiaporphyrinato)zinc **4**. The regioselectivity changed when the reaction temperature was varied: (5-thiaporphyrinato)zinc **4** was formed exclusively in a reaction at 0 °C for 90 min (Table 1). We assumed that the activation energy of formation of (5-oxaporphyrinato)zinc is higher than that of the formation of (5-thiaporphyrinato)zinc, and the formation of **4** is favorable at a low temperature. However, the selectivity of the reaction at 60 °C cannot be explained solely by the difference in the activation energy. The ring-opening reaction of **2** with CH_3COS^- can proceed at 60 °C to lower the yield of **2**.

In order to determine the activation energy of the reaction forming (5-thiaporphyrinato)zinc and (5-oxaporphyrin-ato)zinc, we determined the rates of ring-closure reaction of bilin-1,19-dithione **8** and bilin-1,19-dione **1** at various temperatures. Bilin-1,19-dithione **8** was prepared from (5-thiaporphyrinato)zinc **4** as shown in Scheme 3. Bilin-1,19-dithione **8** (0.01 mM), zinc acetate (0.1 mM) and acetic anhydride (2 mM) in toluene were allowed to react at 10, 30, and 50 °C, and the progress of formation of (5-thiaporphyrinato)zinc **4** was monitored by UV-visible spectroscopy. From the Arrhenius plot of the pseudo-first order rate constants (Fig. S25), the activation energy was determined to be 14.6 kJ mol^{-1}. Similarly, the rate of (5-oxaporphyrinato)zinc **2** formation from bilin-1,19-dione **1** was determined. The activation energy was 34.3 kJ mol^{-1}. These results indicate that the activation energy of formation of (5-thiaporphyrinato)zinc is lower than that of the formation of (5-oxaporphyrinato)zinc.

Plausible mechanism of ring-closing reaction of **3** to form **2** and **4** is initiated by acetylation of O or S to form intermediates A and E (Fig. 1). Then intramolecular nucleophilic attack of O or S resulted in the formation of intermediates C and G. Dissociation of AcO or AcS leads to the final products D and H. We performed quantum chemical calculations[34] of transformation

Table 1 Yields and selectivity of the ring-closure reaction of 19-thioxobilin-1-one **3** to afford *meso*-heteroatom porphyrins **2** or **4**

	(5-Oxaporphyrinato) zinc **2** (%)	(5-Thiaporphyrinato) zinc **4** (%)
60 °C, 30 min	31	45
rt, 30 min	39	40
0 °C, 90 min	Trace	78

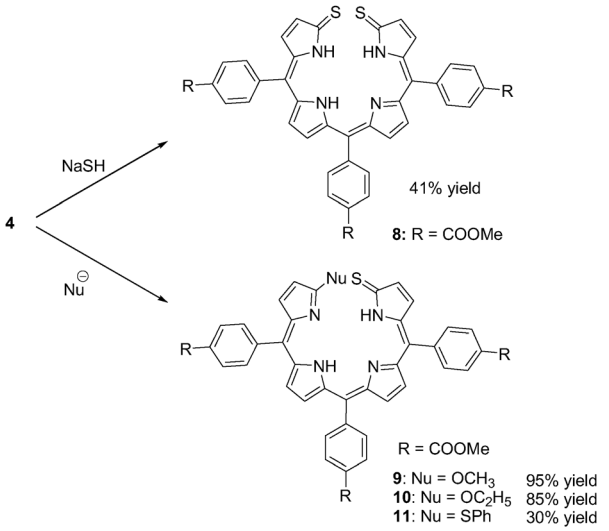

Scheme 3 Preparation of 19-substituted bilin-1-thiones **8–11**.

from 19-acetoxybilin-1-thione or 19-acetylthiobilin-1-one to (5-thia- or 5-oxaporphyrinato)zinc. In Fig. 1 are shown the total energies of 19-acetoxybilin-1-thione or 19-acetylthiobilin-1-one (structures between A and C or E and G, Fig. 1) with the distance between S or O atoms and C-19 varied. Similarly, the total energies of the tetrahedral intermediates (structures between C and D or G and H, Fig. 1) with the distance between C-19 and O or S atoms varied are shown in Fig. 1. The distance between S and C-19 in the transition state (B, Fig. 1) was 2.36 Å. The distance between O and C-19 in the transition state for the formation of (5-oxaporphyrinato)zinc (F, Fig. 1) was 1.85 Å. The transition states B and F have a single imaginary frequency of 239.0i cm^{-1} and 394.8i cm^{-1}, respectively. The activation energy of (5-thiaporphyrinato)zinc formation was lower than that of (5-oxaporphyrinato)zinc. These results support our assumption that the temperature dependence of regioselectivity of the reaction shown in Scheme 2 is ascribed to a difference in the activation energies. According to the quantum chemical calculations, the formation of (5-thiaporphyrinato)zinc is exothermic, while the formation of (5-oxaporphyrinato)zinc is not.

The DFT-optimized structures of bilindithione **8** and bilindione **1** are shown in Fig. 2. Both compounds adopt a helical conformation. The distance between thiocarbonyl carbons was larger than that between the carbonyl carbons. The helical pitch of bilinthione **8** is greater than that of bilindione **1**.

Spectroscopic properties of (5-thiaporphyrinato)zinc

Fig. 3 compares the UV-visible spectra of (5-thiaporphyrinato)zinc **4** and (5-oxaporphyrinato)zinc **2**. The UV-visible spectrum of **4** is characterized by an intense Soret band at 433 nm and a weak Q-band at 646 nm. Time dependent density functional theory calculations (B3LYP/6-31+G(D,P)) showed that **4** exhibits absorption at 568.5 nm (f = 0.1896, HOMO → LUMO 61.6%) and 430.9 nm (f = 0.2515, HOMO−3 → LUMO+1, 51.4%). We assigned the Soret band to the latter transition and the Q-band to the former transition. The transition moments of both bands were parallel to a line connecting

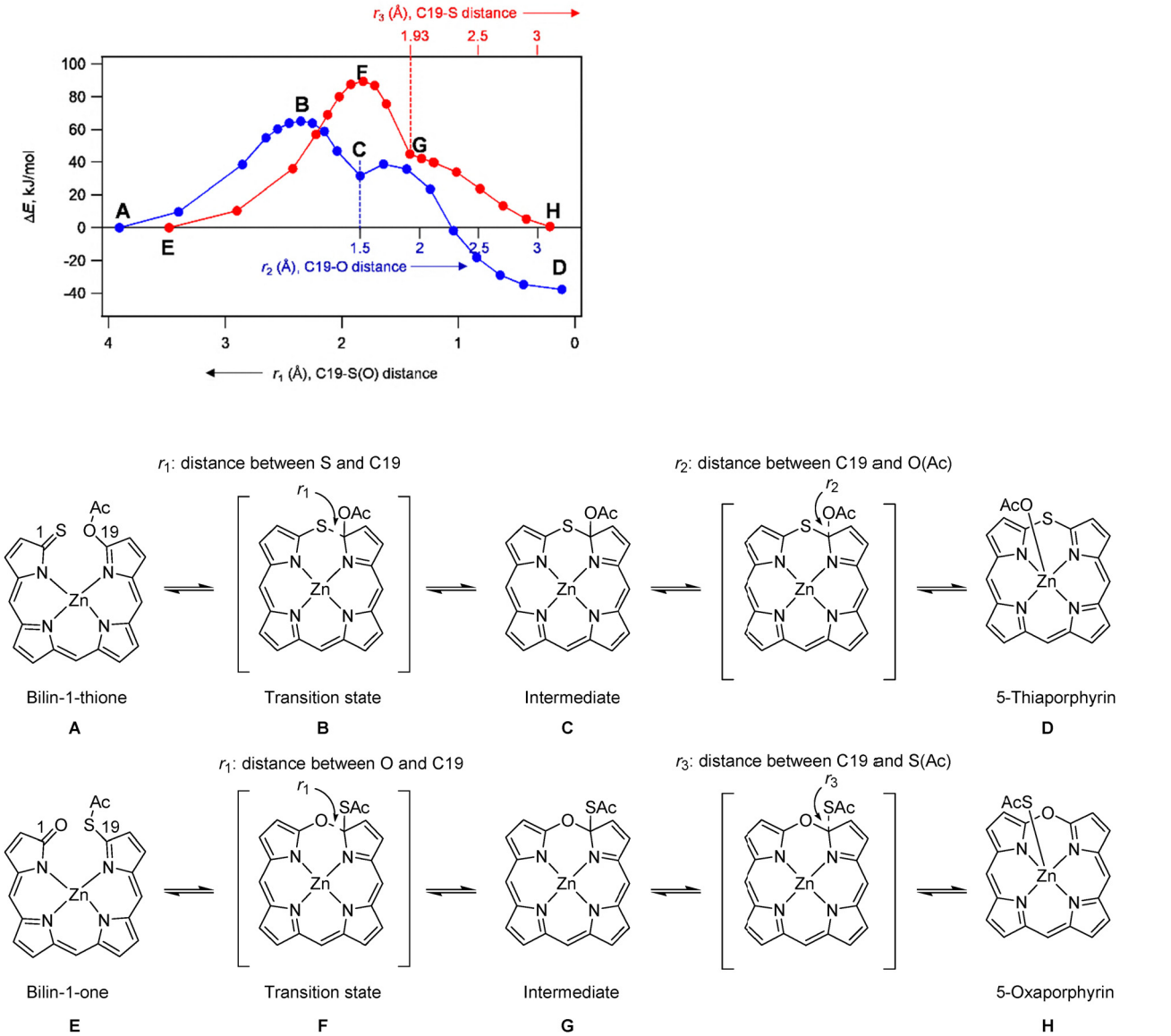

Fig. 1 Energy profiles of transformation of bilin-1-one or bilin-1-thione to an intermediate, and to 5-thia- or (5-oxaporphyrinato)zinc. Energy was calculated with B3LYP/6-31+G(D,P) with optimization of all the coordinates except for r_1, r_2, and r_3.

C10–C20. The UV-visible spectrum of **2** is characterized by a split Soret band at 390 and 411 nm and a Q-band at 646 nm.[18] As shown in Fig. S19, the fluorescence quantum yield of **4** was quite low. The fluorescence quantum yield of (5-thiaporphyrinato)zinc **4** was 0.0016, whereas that of (5-oxaporphyrinato)zinc **2** was 0.071. The low fluorescence quantum yield of (β-octaethyl-5-thiaporphyrinato)zinc was also reported in the literature.[16]

^{1}H NMR and ^{13}C NMR results of **4** are shown in Fig. S1–S4. The HMQC spectrum of **4** revealed that the proton at 8.70 ppm is bonded to the carbon at 136.8 ppm and the proton at 8.84 ppm is bonded to the carbon at 129.5 ppm. According to the quantum chemical calculations, C-3 should have the smallest chemical shift among the pyrrole β-carbons. The ^{1}H–^{1}H COSY spectrum (Fig. S3) indicates that the protons at 8.70 ppm and those at 8.84 ppm are vicinal. Therefore, we assigned the signals at 8.84 and 129.5 ppm to H-3 and C-3, respectively. Signals in the ^{1}H NMR were assigned as shown in Fig. S1. Table 2 compares the chemical shifts of ^{1}H NMR of *meso*-heteroporphyrins with those of the parent porphyrin. The chemical shifts of pyrrole β-protons of (5-thiaporphyrinato)zinc were *ca.* 0.5 ppm downfield shifted compared to those of (5-oxaporphyrinato)zinc. Downfield chemical shifts in (5-thiaporphyrinato)zinc indicate that there is a larger aromatic ring current in (5-thiaporphyrinato)zinc than in (5-oxaporphyrinato)zinc. Nucleus independent chemical shifts (NICS)[35] were calculated for zinc porphine, zinc 5-oxaporphine and zinc 5-thiaporphine. The ghost atom was placed 3 Å above the zinc atom. The values of NICS(3)$_{zz}$ obtained based on the HF/6-311G(D,P) level were −23.3, −10.9, and −13.2 ppm for zinc porphine, zinc 5-oxaporphine and zinc 5-thiaporphine, respectively. These results indicate that the

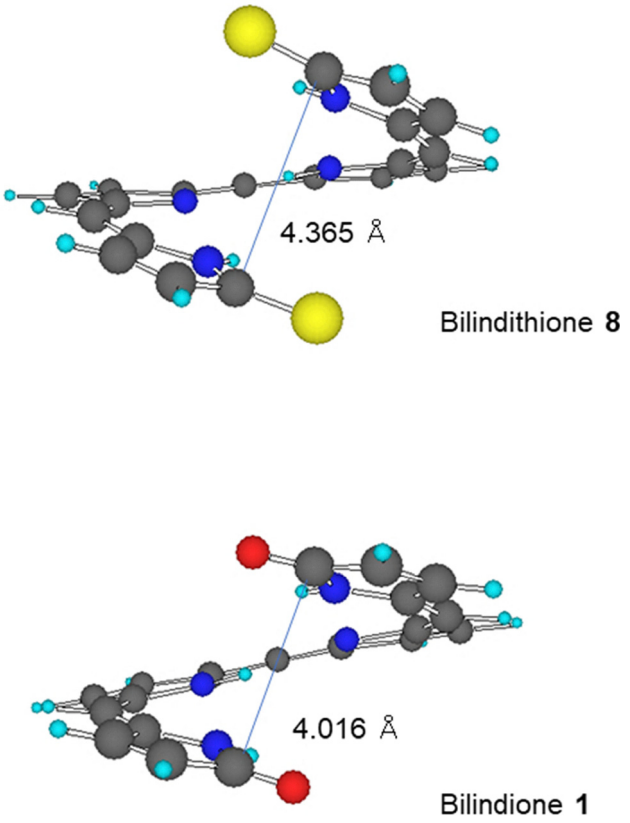

Fig. 2 Comparison of optimized structures of bilindithione 8 and bilindione 1. The structures were optimized with B3LYP/6-31++G(D,P). The distances between C1 and C19 are shown. *meso*-Aryl groups were omitted for calculation.

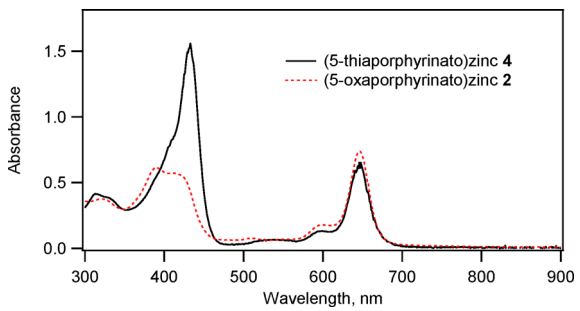

Fig. 3 UV-visible spectra of (5-thiaporphyrinato)zinc **4** and (5-oxaporphyrinato)zinc **2**, 1.35×10^{-5} M in $CHCl_3$.

aromaticity of these porphyrins decreases in the order: zinc porphine ≫ zinc 5-thiaporphine > zinc 5-oxaporphine.

Preparation of 19-substituted bilin-1-thione from (5-thiaporphyrinato)zinc

Ring-opening reaction of (5-thiaporphyrinato)zinc **4** with nucleophiles proceeded with high yields in many cases. For instance, (5-thiaporphyrinato)zinc **4** was reacted with sodium methoxide and sodium ethoxide, giving 19-methoxy- and 19-ethoxybilin-1-thione in 95% and 85% yield, respectively (Scheme 3). On the other hand, the reaction between (5-thiaporphyrinato)zinc **4** and sodium benzenethiolate gave 19-phenylsulfanylbilin-1-thione in 31% yield. Although the ring-opening reaction with sodium benzenethiolate proceeded rapidly, the reverse reaction, the ring-closure reaction also proceeded during the acidic work-up to lower the yield of 19-phenylsulfanylbilin-1-thione. A similar behavior was also observed in the ring-opening reaction of the copper complex of 5-oxaporphyrin **7** to prepare 19-phenoxybilin-1-one **15**.[24] Ring-opening reaction of **7** with phenoxide proceeded rapidly, but a considerable amount of **7** was regenerated during workup. Attempts to prepare 19-phenoxybilin-1-thione by ring-opening of **4** with phenoxide failed, probably because the reverse ring-closing reaction occurred rapidly.

Bilindiones and biliverdins show two bands in the UV-visible spectra at ~380 and ~650 nm.[36] In Fig. 4 are shown the UV-visible spectra of bilin-1,19-dione **1**, 19-thioxobilin-1-one **3**, and bilin-1,19-dithione **8**. The absorption maxima of bilin-1,19-dione **1** (λ_{max} = 401 and 624 nm)[36] were bathochromically shifted to 442 and 672 nm for 19-thioxobilin-1-one **3** and 485 and 726 nm for bilin-1,19-dithione **8**. These three bilins showed absorption bands in different wavelengths, and can be clearly distinguished by UV-visible spectroscopy.

UV-visible spectra of 19-substituted bilin-1-thiones **9–11** are compared with those of the corresponding bilin-1-ones **12–14** (for the structures, see Chart 1) in Fig. 5. The absorption maxima of the B-band of bilin-1-thione were 30–45 nm bathochromically shifted compared with those of bilin-1-ones. Similarly, the absorption maxima of the Q-band of bilin-1-thiones were 31–53 nm bathochromically shifted.

Metal ion templated ring-closing reaction of 19-substituted bilin-1-thione

Balch and coworkers reported that the copper complex of 19-formylbilin-1-one was converted to (5-oxaporphyrinato)copper(II) by the reaction with dioxygen and trifluoroacetic acid.[37] We reported that bilin-1-one having an appropriate leaving group such as C_6H_5O– at the 19-carbon undergoes cyclization to form (5-oxaporphyrinato)zinc or (5-oxaporphyrinato)copper upon the

Table 2 Comparison of chemical shifts (δ/ppm) of ^{1}H NMR and ^{13}C NMR of [5,10,15,20-tetrakis(4-methoxycarbonylphenyl)porphyrinato]zinc, (5-oxaporphyrinato)zinc **2** and (5-thiaporphyrinato)zinc **4**

	[Porphyrinato]zinc	(5-Oxaporphyrinato)zinc **2**	(5-Thiaporphyrinato)zinc **4**
β-Pyrrole H	8.82	7.76, 7.92, 8.09, 8.22	8.29, 8.41, 8.70, 8.84
meso-Phenylene	8.44, 8.3	7.94–8.06, 8.31, 8.34	8.16, 8.38, 8.41
C-2		138.6	136.7
C-3		120.0	129.2
C-12, 13		130.8, 134.5	133.1, 135.4

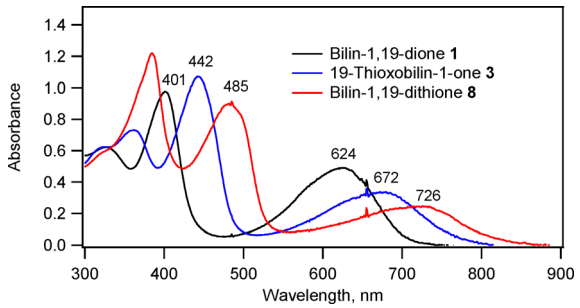

Fig. 4 UV-visible spectra of bilindione, thioxobilinone, and bilindithione, 2 × 10^{-5} M in CH_2Cl_2.

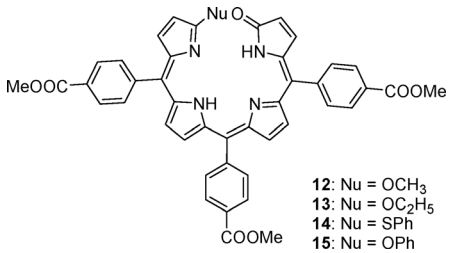

Chart 1 19-Substituted bilin-1-ones.

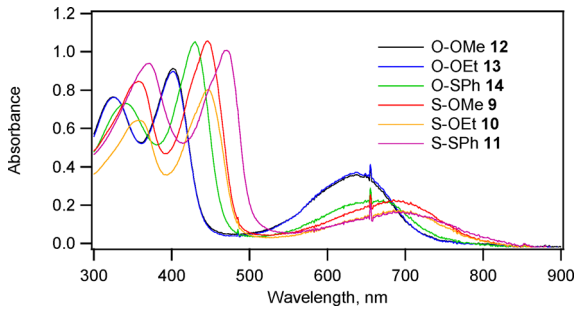

Fig. 5 UV-visible spectra of 19-substituted bilin-1-ones **12–14** and bilin-1-thiones **9–11**. 2 × 10^{-5} M in CH_2Cl_2 at 298 K.

addition of zinc or copper ions under ambient conditions.[38] In order to examine similar condensation–cyclization for the sulfur analogues, we investigated the reaction of bilin-1-thiones **9–11** with various metal acetates.

Fig. 6 shows the UV-visible spectral changes of 19-phenylsulfanylbilin-1-thione **11** upon the addition of zinc acetate. The peaks of bilin-1-thione **11** at 371, 471, and 685 nm decreased with concomitant increase in absorbance at 425 and 638 nm with several isosbestic points. Table 3 lists the rate constants of formation of 5-heteroatom porphyrins from **11**, **14** and **15**. The rate constant of the ring-closing reaction of 19-phenylsulfanylbilin-1-thione **11** in the presence of zinc acetate is 10^4 times greater than that of 19-phenylsulfanylbilin-1-one **14**, demonstrating higher nucleophilicity of sulfur than oxygen. Pearson *et al.* reported that the ratio of the rate constant of nucleophilic substitution of iodomethane with benzenethiolate

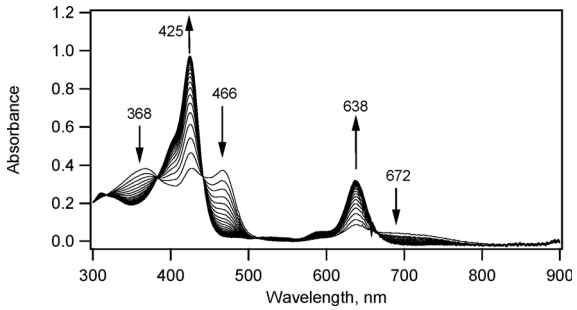

Fig. 6 UV-visible spectral changes of 1 × 10^{-5} M 19-phenylsulfanylbilin-1-thione **11** and 0.1 mM zinc acetate in 50%(v/v) acetonitrile in water at 298 K. Spectra were recorded every 4 seconds.

to that with phenolate is 14 700.[39] Thus, a 10 000-fold acceleration can reasonably be attributed to the difference in nucleophilicity.

The reaction proceeds *via* two steps as shown in Scheme 4.[38] Bilin-1-thione forms a metal complex followed by cyclization to (5-thiaporphyrinato)zinc. The spectral changes shown in Fig. 6 are different from those observed for the reaction of 19-phenoxybilin-1-one **15** with zinc acetate.[38] For the reaction of **15**, rapid increase in a band at 800 nm due to the zinc complex of 19-phenoxybilin-1-one was observed initially, followed by subsequent increase in a band at 650 nm due to (5-oxaporphyrinato)zinc with concomitant decrease in the 800 nm band. This spectral change indicates that the first step in Scheme 4, the metal complex formation step, is faster than the second cyclization step. In contrast, the spectral changes observed for the reaction between **11** and $Zn(OAc)_2$ shown in Fig. 6 indicate that formation of the zinc complex of **11** was not detected in the UV-visible spectra. Therefore, the cyclization step is faster than the metal complexation step of bilin-1-thione **11**. It is noteworthy that Mg^{2+}, Ni^{2+}, and Cd^{2+} also induced cyclization of **11**, while these metal ions cannot induce cyclization of **14** or **15**. The metal complexes of 5-thiaporphyrins were characterized by MALDI-TOF mass spectroscopy (Fig. S20–S24). The computer-simulated patterns for the composition are identical to the experimental patterns, supporting the formation of the metal complexes. The UV-visible spectra of these complexes are shown in Fig. S18. The absorption maxima of the B-band of the zinc, cobalt, nickel and magnesium complexes of 5-thiaporphyrin were 425 nm, while those of the copper complex and the cadmium complex were 420 and 434 nm, respectively. The absorption maxima of the Q-band of the zinc, copper, cobalt, nickel and magnesium complexes of 5-thiaporphyrin were 637–639 nm, while that of the cadmium complex was 644 nm. 19-Methoxybilin-1-thione **9** also reacts with copper(II) acetate to form (5-thiaporphyrinato)copper slowly, the half-life of the reaction being approximately 2 h. Balch and coworkers reported that 19-methoxyoctaethylbilin-1-one is converted to the 5-oxaporphyrin cobalt complex upon the addition of Co(II).[40]

Conclusions

We elucidated how the reaction rate for the formation of 5-thiaporphyrin from a linear tetrapyrrole bearing a thioketo

Table 3 The first-order rate constants of the ring-closure reaction of 19-phenylsulfanylbilin-1-thione **11** (0.01 mM) and various metal acetates (0.1 mM) in 50% (v/v) acetonitrile-water at 298 K

	k [s^{-1}]		
	19-Phenylsulfanylbilin-1-thione **11**	19-Phenylsulfanylbilin-1-one **14**[38]	19-Phenoxybilin-1-one **15**[38]
Cu^{2+}	>0.1	$(2.5 \pm 0.2) \times 10^{-2}$	$(1.0 \pm 0.1) \times 10^{-1}$
Zn^{2+}	$(4.4 \pm 0.1) \times 10^{-2}$	$(4.0 \pm 0.2) \times 10^{-6}$	$(1.3 \pm 0.1) \times 10^{-3}$
Co^{2+}	$(1.24 \pm 0.06) \times 10^{-4}$		$(1.3 \pm 0.2) \times 10^{-4}$
Cd^{2+}	$(5.5 \pm 0.2) \times 10^{-3}$		
Ni^{2+}	$(5.8 \pm 0.2) \times 10^{-5}$		
Mg^{2+}	$(2.24 \pm 0.03) \times 10^{-5}$		

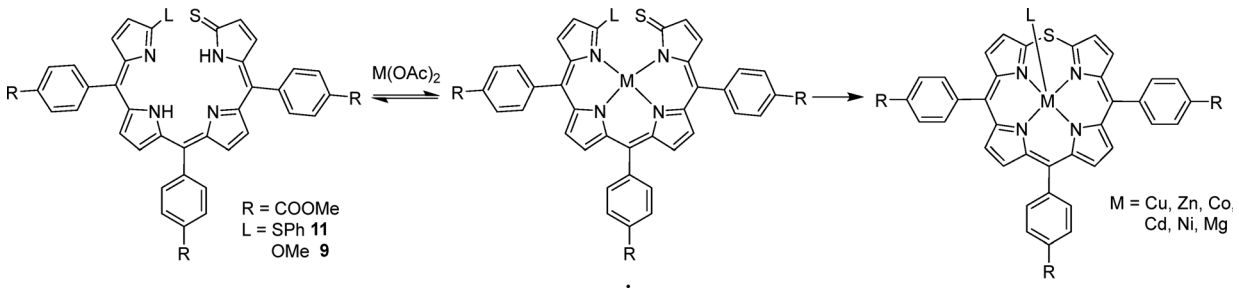

Scheme 4 Metal ion templated ring-closing reaction of 19-substituted bilin-1-thione **11** or **9**.

group differs from that for the formation of 5-oxaporphyrin from a linear tetrapyrrole bearing a keto group. In addition, the spectral properties of thiaporphyrin and the linear tetrapyrrole containing a thioketo group, including their ^{1}H- and ^{13}C-NMR spectra and UV-visible absorption spectra, were also examined. The reaction of 19-thioxobilin-1-one with acetic anhydride and zinc acetate afforded two products, (5-thiaporphyrinato)zinc and (5-oxaporphyrinato)zinc. Formation of (5-thiaporphyrinato)zinc was favored at a low temperature. The activation energy of cyclization to afford (5-thiaporphyrinato)zinc was lower than that of cyclization to afford (5-oxaporphyrinato)zinc. Compared to (5-oxaporphyrinato)zinc, the UV-visible spectrum of (5-thiaporphyrinato)zinc was closer to that of porphyrin. The linear tetrapyrroles with a thioketo group showed unique reactivity. Metal ion induced-cyclization of 19-substituted bilin-1-thione proceeded faster than that of 19-substituted bilin-1-one. The rate constant of the reaction between 19-phenylsulfanylbilin-1-thione and zinc ion was 10^4 larger than that between 19-phenylsulfanylbilin-1-one and zinc ion. We demonstrated that 5-thiaporphyrin is thermodynamically stable and bilin-1-thione is kinetically labile compared to their oxygen counterparts.

Experimental

Bilindione **1** and biladienone **6** were prepared according to ref. 19 and 23, respectively. 5-Oxaporphyrins **2** and **7** were prepared according to ref. 18 and 24, respectively. Bilinone **3** was prepared from **2** according to ref. 31 or from **5** as described in the SI. Bilin-1-ones with a substituent at 19 position **12–15** were prepared according to the published procedure.[31]

[21,23-Didehydro-10,15,20-tris(4-methoxycarbonylphenyl)-23*H*-5-thiaporphyrinato](trifluoroacetato) zinc(II) 4

A solution of (4*Z*,9*Z*,15*Z*)-5,10,15-Tris(4-methoxycarbonylphenyl)-(21*H*,23*H*,24*H*)-19-thioxo-1,19,21,24-tetrahydrobilin-1-one **3** 233 mg (0.431 mmol) and zinc acetate 135 mg (0.733 mmol, 1.7 eq) in amylene-stabilized chloroform 100 mL was cooled in an ice-water bath, and acetic anhydride 8.16 mL (86.3 mmol, 200 eq) was added. The mixture was stirred for 1 h in an ice-water bath. The chloroform solution was washed with water twice. After drying over Na_2SO_4, evaporation of the solvent afforded a green solid. It was purified with silica gel column (CH_2Cl_2 : acetone : TFA = 20 : 1 : 0.1). The first fraction was 5-oxaporphyrin, and the second blue-green fraction was collected. Evaporation of the solvent yielded 305.7 mg (0.341 mmol, 79%) of (5-thiaporphyrinato)zinc **4**.

^{1}H NMR (500 MHz, $CDCl_3$) δ/ppm: 4.08 (s, 3H), 4.10 (s, 6H), 8.16 (br. d, J = 8 Hz, 6H), 8.29 (d, J = 4.6 Hz, 2H), 8.38 (d, J = 8 Hz, 2H), 8.411 (d, J = 5.2 Hz, 2H), 8.414 (d, J = 8 Hz, 4H), 8.70 (d, J = 5.2 Hz, 2H, H-2), 8.84 (d, J = 4.6 Hz, 2H, H-3). ^{13}C NMR (126 MHz, $CDCl_3$) δ/ppm: 52.5 (OCH_3), 52.6 (OCH_3), 127.9 (phenylene meta), 128.2 (phenylene meta), 129.2 (pyrrole C-3), 130.5, 130.6, 132.1, 133.1 (pyrrole C-12), 133.5 (phenylene ortho), 133.6 (phenylene ortho), 135.4 (pyrrole C-13), 136.7 (pyrrole C-2), 136.8, 144.7, 145.2, 148.9, 151.5, 154.3, 155.6, 166.9, 166.9. MS (MALDI-TOF): calcd for $C_{43}H_{29}O_6N_4SZn$ ([**4** – CF_3COO]$^+$) m/z = 793.11; found 793.15. UV-visible (CH_2Cl_2, 25 °C): λ_{max} (ε_{max}) 431 nm (1.06×10^5 M^{-1} cm^{-1}), 644 nm (4.06×10^4 M^{-1} cm^{-1}). Anal. Calcd for $C_{45}H_{29}F_3N_4O_8SZn \cdot 2.4H_2O$: C, 56.52; H, 3.56; N, 5.86; S, 3.35. Found: C, 56.51; H, 3.09; N, 5.87; S, 3.24.

(4*Z*,9*Z*,15*Z*)-1,21-Dihydro-19-methoxy-5,10,15-tris(4-methoxycarbonylphenyl)-23*H*-bilin-1-thione 9

To (5-thiaporphyrinato)zinc **4** 30 mg (0.033 mmol) was added a solution of sodium methoxide 7.7 mg (0.142 mmol, 4.3 eq) in dry methanol (5 mL). The mixture was stirred for 5 min at room temperature. Aqueous NH_4Cl (10%, 20 mL) was added and the solution was stirred for 5 min. Chloroform (100 mL) was added and the solution was washed with 10% aqueous NH_4Cl, 1 M HCl, and saturated aqueous NaCl. The chloroform layer was dried over Na_2SO_4 and the solvent was evaporated. Purification with silica gel column ($CHCl_3$) afforded a green solid of **9** 23.9 mg (0.031 mmol, 95%).

^{1}H NMR (500 MHz, $CDCl_3$) δ/ppm: 3.10 (s, 3H), 4.00 (m, 9H), 5.86 (d, J = 4.6 Hz, 1H), 6.56 (dd, J_1 = 4.6 Hz, J_2 =2.3 Hz, 1H), 6.71 (dd, J_1 = 5.2 Hz, J_2 = 2.3 Hz, 1H), 6.75–6.85 (1H), 6.88 (d, J = 4.6 Hz, 1H), 6.97 (d, J = 4.6 Hz, 1H), 7.16 (d, J = 4.6 Hz, 1H), 7.36 (d, J = 4.6 Hz, 1H), 7.63–7.71 (m, 6H), 8.18–8.22 (m, 6H), 9.92 (s, 1H), 11.30 (s, 1H). ^{13}C NMR (126 MHz, $CDCl_3$) δ/ppm: 52.3, 52.4, 55.2, 117.7, 119.2, 120.6, 125.2, 128.6, 128.8, 129.1, 129.6, 130.1, 130.2, 131.0, 131.5, 131.6, 132.4, 133.0, 134.5, 137.2, 137.7, 138.6, 141.5, 141.7, 142.3, 142.6, 146, 147.9, 152.1, 163.8, 166.7, 166.9, 177.3, 188.2 (C═S). MS (MALDI-TOF) m/z: calcd for $C_{44}H_{35}N_4O_7S$ ([**9** + H]$^+$) 763.22; found 763.39. UV-visible (CH_2Cl_2, 25 °C): λ_{max} (ε_{max}) 357 nm (4.23×10^4 M^{-1} cm^{-1}), 446 nm (5.28×10^4 M^{-1} cm^{-1}), 691 nm (1.12×10^4 M^{-1} cm^{-1}).

(4*Z*,9*Z*,15*Z*)-1,21-Dihydro-19-ethoxy-5,10,15-tris(4-methoxycarbonylphenyl)-23*H*-bilin-1-thione 10

To (5-thiaporphyrinato)zinc **4** 30 mg (0.033 mmol) was added a solution of sodium ethoxide 9.7 mg (0.142 mmol, 4.3 eq) in amylene-stabilized chloroform (100 mL). The mixture was stirred for 30 min at room temperature. 10% aqueous NH_4Cl (200 mL) was added and the solution was stirred for 5 min. The organic layer was washed with 10% aqueous NH_4Cl, 1 M HCl, and saturated aqueous NaCl. The chloroform layer was dried over Na_2SO_4 and the solvent was evaporated. The residue was purified with silica gel column chromatography eluted with chloroform to afford a green solid of **10** in 21.9 mg (0.028 mmol, 85%) yield.

^{1}H NMR (500 MHz, $CDCl_3$) δ/ppm: 0.87 (t, J = 7.2 Hz, 3H) 3.07–3.71 (bd, J = 16.4 Hz, 2H), 3.95–4.02 (m, 9H; $COOCH_3$), 5.85 (d, J = 4.6 Hz, 1H), 6.53 (t, J = 2.3 Hz, 1H), 6.72 (d, J = 5.2 Hz, 1H), 6.77 (s, 1H), 6.88 (d, J = 4.6 Hz, 1H), 6.96 (d, J = 5.2 Hz, 1H), 7.15 (d, J = 4.0 Hz, 1H), 7.37 (d, J = 5.2 Hz, 1H), 7.68 (dd, J = 16.9, 7.7 Hz, 6H), 8.22–8.18 (m, 6H), 9.96 (s, 1H; NH), 11.30 (s, 1H; NH). ^{13}C NMR (126 MHz, $CDCl_3$) δ/ppm: 13.5, 51.3, 51.4, 63.2, 116.7, 118.5, 119.5, 124.2, 127.4, 127.5, 128.1, 128.5, 129.1, 129.1, 130.0, 130.5, 130.8, 131.4, 131.9, 133.4, 136.2, 136.7, 137.4, 140.6, 141.4, 141.8, 145.0, 147.1, 151.0, 162.8, 165.6, 165.7, 165.9, 175.9, 187.1 (C═S). MS (MALDI-TOF) m/z: calcd for $C_{45}H_{37}N_4O_7S$ ([**10** + H]$^+$) 777.24; found 777.38. UV-visible (CH_2Cl_2, 25 °C): λ_{max} (ε_{max}) 358 nm (3.21×10^4 M^{-1} cm^{-1}), 446 nm (4.02×10^4 M^{-1} cm^{-1}), 685 nm (8.76×10^3 M^{-1} cm^{-1}).

(4*Z*,9*Z*,15*Z*)-1,21-Dihydro-5,10,15-tris(4-methoxycarbonylphenyl)-19-phenylsulfanyl-23*H*-bilin-1-thione 11

To a solution of (5-thiaporphyrinato)zinc **4** 36.3 mg (0.04 mmol) in dry dichloromethane (20 mL) was added a solution of benzenethiol 32.8 μL (0.32 mmol, 8 eq) and sodium hydride 60% oil dispersion 44.8 mg (1.12 mmol, 28 eq) in dry THF. The mixture was stirred for 12 h at room temperature. The reaction mixture was washed with water, aqueous 1 M HCl, and water. After the organic layer was dried over Na_2SO_4, the solvent was evaporated to afford a green solid. It was purified with silica gel column using chloroform as an eluant. The first green fraction was collected, and evaporation of the solvent yielded 10.3 mg (0.012 mmol, 30.5%) of the desired bilinthione **11**.

^{1}H NMR (500 MHz, CD_2Cl_2) δ/ppm: 3.97–3.94 (m, 9H; $COOCH_3$), 5.79 (d, J = 4.6 Hz, 1H), 6.53 (d, J = 4.6 Hz, 1H), 6.78 (d, J = 2.0 Hz, 1H), 6.92 (q, J = 1.9 Hz, 1H), 6.95 (d, J = 4.6 Hz, 1H), 7.02 (d, J = 4.6 Hz, 1H), 7.26–7.34 (m, 5H), 7.46 (d, J = 5.2 Hz, 1H), 7.76–7.82 (m, 6H), 8.15–8.22 (m, 6H), 9.75 (s, 1H), 11.25 (s, 1H). ^{13}C NMR (126 MHz, $CDCl_3$) δ/ppm: 52.3, 52.4, 118.1, 122.1, 124.3, 124.6, 129.1, 129.2, 129.2, 129.4, 129.6, 129.8, 129.9, 130.4, 130.8, 131.0, 131.5, 131.7, 131.8, 132.8, 133.6, 134.4, 134.8, 136.1, 136.2, 138.6, 141.4, 141.6, 142.0, 142.4, 145.5, 151.6, 152.9, 165.2, 166.7, 166.8, 166.8, 173.8, 188.8 (C═S). MS (MALDI-TOF): m/z: calcd for $C_{49}H_{37}N_4O_6S_2$ ([**11** + H]$^+$) 841.21; found 841.27. UV-visible (CH_2Cl_2, 25 °C): λ_{max} (ε_{max}) 371 nm (4.70×10^4 M^{-1} cm^{-1}), 471 nm (5.04×10^4 M^{-1} cm^{-1}), 685 nm (8.42×10^3 M^{-1} cm^{-1}).

(4*Z*,9*Z*,15*Z*)-1,21-Dihydro-5,10,15-tris(4-methoxycarbonylphenyl)-23*H*-bilin-1,19-dithione 8

To a solution of (5-thiaporphyrinato)zinc **4** 150 mg (0.165 mmol) in acetone 200 mL was added an aqueous solution of NaSH (2.6 M, 1.18 mL, 3.07 mmol, 18.6 eq), and the mixture was stirred at room temperature for 30 sec. Chloroform (200 mL) was added and the organic layer was washed with aqueous 1 M HCl and saturated aqueous NaCl. The organic layer was dried over Na_2SO_4 and evaporation of the solvent afforded a green solid. It was purified with silica gel column eluted with chloroform. The first green fraction was discarded, and the second green fraction was collected. Evaporation of the solvent afforded 50.0 mg (0.0654 mmol, 40%) of bilindithione **8**.

^{1}H NMR (500 MHz, $CDCl_3$) δ/ppm: 3.99 (s, 3H; CH_3),4.01 (s, 6H; CH_3), 6.46 (d, J = 5.2 Hz, 2H), 7.00 (d, J = 4.0 Hz, 2H), 7.34 (d, J = 4.0 Hz, 2H), 7.41 (d, J = 5.2 Hz, 2H), 7.67 (d, J = 8.0 Hz, 4H), 7.84 (d, J = 8.0 Hz, 2H), 8.20 (d, J = 8.6 Hz, 4H), 8.28 (d, J = 8.6 Hz, 2H). ^{13}C NMR (126 MHz, $CDCl_3$) δ/ppm: 52.5, 52.6, 118.1, 125.8, 129.2, 129.6, 129.7, 130.6, 130.9, 131.0, 131.2, 131.3, 131.3, 132.2, 132.3, 134.4, 141.0, 141.2, 143.1, 166.7, 166.8, 187.8 (C═S). MS (MALDI-TOF) m/z: calcd for $C_{43}H_{33}N_4O_6S_2$ ([**8** + H]$^+$) 765.18; found 765.24. UV-visible (CH_2Cl_2, 25 °C): λ_{max} (ε_{max}) 385 nm (6.10×10^4 M^{-1} cm^{-1}), 485 nm (4.57×10^4 M^{-1} cm^{-1}), 726 nm (1.23×10^4 M^{-1} cm^{-1}).

Author contributions

Hideki Uno: writing – original draft, investigation, visualization. Muneki Hayakawa: investigation, visualization. Akuto Takagi: investigation, supervision. Tadashi Mizutani: conceptualization, writing – original draft, writing – reviews & editing, investigation, supervision.

Conflicts of interest

There are no conflicts to declare.

Data availability

All data included in this study are available upon request by contact with the corresponding author.

Supplementary information: Preparation of **3** from **7**, NMR and mass spectra of (5-thiaporphyrinato)zinc and bilin-1-thiones, UV-visible spectra and mass spectra of the metal complexes of 5-thiaporphyrin, fluorescence emission spectra of **2** and **4**, the Arrhenius plot of formation of **2** or **4**, and optimized structures of A–H in Fig. 1. HOMO/LUMO energy levels of (porphinato)zinc, (5-azaporphinato)zinc, (5-oxaporphinato)(trifluoroacetato)zinc, and (5-thiaporphinato)(trifluoroacetato)zinc calculated at the B3LYP/6-31G(D) level. See DOI: **https://doi.org/10.1039/d5nj02301g**.

References

1 P. R. Ortiz De Montellano, Heme Oxygenase Mechanism: Evidence for an Electrophilic, Ferric Peroxide Species, *Acc. Chem. Res.*, 1998, **31**, 543–549.
2 D. J. Schuller, A. Wilks, P. R. O. de Montellano and T. L. Poulos, Crystal structure of human heme oxygenase-1, *Nat. Struct. Biol.*, 1999, **6**, 860–867.
3 G. Kikuchi, T. Yoshida and M. Noguchi, Heme oxygenase and heme degradation, *Biochem. Biophys. Res. Commun.*, 2005, **338**, 558–567.
4 Y. Matano, Synthesis of Aza-, Oxa-, and Thiaporphyrins and Related Compounds, *Chem. Rev.*, 2017, **117**, 3138–3191.
5 A. Urban and S. De Feyter, Making and Breaking Helical Open-Chain Oligopyrroles, *ChemPlusChem*, 2024, **89**, e202300708.
6 J. A. Johnson, M. M. Olmstead, A. M. Stolzenberg and A. L. Balch, Ring-opening and Meso Substitution from the Reaction of Cyanide Ion with Zinc Verdoheme, *Inorg. Chem.*, 2001, **40**, 5585.
7 H. Falk, *The Chemistry of Linear Oligopyrroles and Bile Pigments*, Springer-Verlag, Vienna, New York, 1989.
8 J. Y. Takemoto, C. T. Chang, D. Chen and G. Hinton, Heme-Derived Bilins, *Isr. J. Chem.*, 2019, **59**, 378.
9 K. G. Chernov, T. A. Redchuk, E. S. Omelina and V. V. Verkhusha, Near-Infrared Fluorescent Proteins, Biosensors, and Optogenetic Tools Engineered from Phytochromes, *Chem. Rev.*, 2017, **117**, 6423.
10 T. Mizutani, N. Sakai, S. Yagi, T. Takagishi, S. Kitagawa and H. Ogoshi, Allosteric Chirality Amplification in Zinc Bilinone Dimer, *J. Am. Chem. Soc.*, 2000, **122**, 748–749.
11 E. Matsui, N. N. Matsuzawa, O. Harnack, T. Yamauchi, T. Hatazawa, A. Yasuda and T. Mizutani, A New Molecular Switch Based on Helical Biladienone, *Adv. Mater.*, 2006, **18**, 2523–2528.
12 J. Wang, F. Ma, H. Sun, J. Zhang and J. Zhang, Three bilindione isomers: synthesis, characterization and reactivity of biliverdin analogs, *J. Biol. Inorg. Chem.*, 2017, **22**, 727.
13 T. Mizutani and S. Yagi, Linear tetrapyrroles as functional pigments in chemistry and biology, *J. Porphyrins Phthalocyanines*, 2004, **8**, 226–237.
14 R. L. N. Harris, A meso thiaporphyrin, *Tetrahedron Lett.*, 1969, **10**, 3689–3692.
15 M. J. Broadhurst, R. Grigg and A. W. Johnson, Sulphur ExtrusionReactions Applied to the Synthesis of Corroles and Related Systems, *J. Chem. Soc., Perkin Trans. 1*, 1972, 1124–1135.
16 A. Takiguchi, N. Inai, S. Kang, M. Hagai, S. Lee, T. Yanai, D. Kim and H. Shinokubo, 5-Thiaporphyrinium cation: effect of sulphur incorporation on excited state dynamics, *Chem. Commun.*, 2022, **58**, 5956.
17 J. H. Fuhrhop, P. Krüger and W. S. Sheldrick, Preparation, structure and properties of 5-aza-, 5-oxonia-, and 5-thioniamesoporphins dimethyl esters and protoporphin dimethyl esters, *Justus Liebigs Ann. Chem.*, 1977, 339–359.
18 K. Kakeya, A. Nakagawa, T. Mizutani, Y. Hitomi and M. Kodera, Synthesis, Reactivity, and Spectroscopic Properties of meso-Triaryl-5-oxaporphyrins, *J. Org. Chem.*, 2012, **77**, 6510–6519.
19 T. Yamauchi, T. Mizutani, K. Wada, S. Horii, H. Furukawa, S. Masaoka, H. Chang and S. Kitagawa, A Facile and Versatile Preparation of Bilindiones and Biladienones from Tetraarylporphyrins, *Chem. Commun.*, 2005, 1309–1311.
20 R. Nakamura, K. Kakeya, N. Furuta, E. Muta, H. Nishisaka and T. Mizutani, Synthesis of para- or ortho-Substituted Triarylbilindiones and Tetraarylbiladienones by Coupled Oxidation of Tetraarylporphyrins, *J. Org. Chem.*, 2011, **76**, 6108–6115.
21 T. Mizutani, Coupled oxidation of iron tetraarylporphyrins as a synthetic tool for linear tetrapyrroles, *J. Porphyrins phthalocyanines*, 2016, **20**, 108–116.
22 K. Kakeya, A. Shimizu, K. Akasaka and T. Mizutani, Substituent effects on selectivity of coupled oxidation of iron tetraphenylporphyrins, *J. Porphyrins phthalocyanines*, 2015, **19**, 726–733.
23 N. Asano, S. Uemura, T. Kinugawa, H. Akasaka and T. Mizutani, Synthesis of Biladienone and Bilatrienone by Coupled Oxidation of Tetraarylporphyrins, *J. Org. Chem.*, 2007, **72**, 5320–5326.
24 K. Shimada and T. Mizutani, Synthesis and reactivity of 10,15,20-triaryl-5-oxaporphyrin copper complexes, *Tetrahedron Lett.*, 2022, **103**, 153977.
25 B. Evans, K. M. Smith and J. A. S. Cavaleiro, Bile Pigment Studies. Part 4. Some Novel Reactions of Metalloporphyrins with Thallium(III) and Cerium(IV) Salts. Ring Cleavage of meso-Tetraphenylporphyrin, *J. Chem. Soc., Perkin Trans. 1*, 1978, 768–773.
26 J. A. S. Cavaleiro, M. J. E. Hewlins, A. H. Jackson and G. P. M. S. Neves, Structures of the Ring-opened Oxidation Products from meso-Tetraphenylporphyrin, *J. Chem. Soc., Chem. Commun.*, 1986, 142–144.
27 C. Jeandon, B. Krattinger, R. Ruppert and H. J. Callot, Biladienones from the Photooxidation of a meso-gem-Disubstituted Phlorin: Crystal and Molecular Structures of the 3N + O Coordinated Nickel(II) and Copper(II) Complexes, *Inorg. Chem.*, 2001, **40**, 3149–3153.

28 O. Ongayi, M. G. H. Vicente, Z. Ou, K. M. Kadish, M. R. Kumar, F. R. Fronczek and K. M. Smith, Synthesis and Electrochemistry of Undeca-substituted Metallobenzoylbiliverdins, *Inorg. Chem.*, 2006, **45**, 1463–1470.

29 C. Liu, D. Shen and Q. Chen, Unexpected bromination ring-opening of tetraarylporphyrins, *Chem. Commun.*, 2006, 770–772.

30 A. Lashgari, X. Wang, J. A. Krause, S. Sinha and J. Jiang, Electrosynthesis of Verdoheme and Biliverdin Derivatives Following Enzymatic Pathways, *J. Am. Chem. Soc.*, 2024, **146**, 15955.

31 K. Kakeya, M. Aozasa, T. Mizutani, Y. Hitomi and M. Kodera, Nucleophilic Ring Opening of meso-Substituted 5-Oxaporphyrin by Oxygen, Nitrogen, Sulfur, and Carbon Nucleophiles, *J. Org. Chem.*, 2014, **79**, 2591–2600.

32 J. H. Fuhrhop, S. Besecke, J. Subramanian, C. Mengersen and D. Riesner, Reactions of oxophlorines and their π radicals, *J. Am. Chem. Soc.*, 1975, **97**, 7141.

33 S. Saito, S. Sumita, K. Iwai and H. Sano, Preparation of mesoverdohemochrome IX.alpha. dimethyl ester and Mössbauer Spectra of Related Porphyrins, *Bull. Chem. Soc. Jpn.*, 1988, **61**, 3539–3547.

34 M. J. Frisch, G. W. Trucks, H. B. Schlegel, G. E. Scuseria, M. A. Robb, J. R. Cheeseman, G. Scalmani, V. Barone, B. Mennucci, G. A. Petersson, H. Nakatsuji, M. Caricato, X. Li, H. P. Hratchian, A. F. Izmaylov, J. Bloino, G. Zheng, J. L. Sonnenberg, M. Hada, M. Ehara, K. Toyota, R. Fukuda, J. Hasegawa, M. Ishida, T. Nakajima, Y. Honda, O. Kitao, H. Nakai, T. Vreven, J. A. Montgomery, J. E. Peralta, F. Ogliaro, M. Bearpark, J. J. Heyd, E. Brothers, K. N. Kudin, V. N. Staroverov, R. Kobayashi, J. Normand, K. Raghavachari, A. Rendell, J. C. Burant, S. S. Iyengar, J. Tomasi, M. Cossi, N. Rega, J. M. Millam, M. Klene, J. E. Knox, J. B. Cross, V. Bakken, C. Adamo, J. Jaramillo, R. Gomperts, R. E. Stratmann, O. Yazyev, A. J. Austin, R. Cammi, C. Pomelli, J. W. Ochterski, R. L. Martin, K. Morokuma, V. G. Zakrzewski, G. A. Voth, P. Salvador, J. J. Dannenberg, S. Dapprich, A. D. Daniels, O. Farkas, J. B. Foresman, J. V. Ortiz, J. Cioslowski and D. J. Fox, *Gaussian 09, Revision A.02*, 2009.

35 H. Fallah-Bagher-Shaidaei, C. S. Wannere, C. Corminboeuf, R. Puchta and P. V. R. Schleyer, Which NICS Aromaticity Index for Planar π Rings Is Best?, *Org. Lett.*, 2006, **8**, 863.

36 M. Taniguchi and J. S. Lindsey, Absorption and fluorescence spectra of open-chain tetrapyrrole pigments-bilirubins, biliverdins, phycobilins, and synthetic analogues, *J. Photochem. Photobiol., C*, 2023, **55**, 100585.

37 R. Koerner, M. M. Olmstead, A. Ozarowski, S. L. Phillips, P. M. V. Calcar, K. Winkler and A. L. Balch, Possible Intermediates in Biological Metalloporphyrin Oxidative Degradation. Nickel, Copper, and Cobalt Complexes of Octaethylformybiliverdin and Their Conversion to a Verdoheme, *J. Am. Chem. Soc.*, 1998, **120**, 1274.

38 K. Kakeya, H. Fukagawa, A. Teraoka and T. Mizutani, Ring Closure Reaction of 19-Substituted Bilinones to 5-Oxaporphyrin Metal Complexes Induced by Zn^{2+} and Cu^{2+}-Application to Turn-on Red Fluorogenic Probes for Zinc Ions-, *Chem. Lett.*, 2021, **50**, 908–911.

39 R. G. Pearson, H. R. Sobel and J. Songstad, Nucleophilic reactivity constants toward methyl iodide and trans-dichlorodi(pyridine)platinum(II), *J. Am. Chem. Soc.*, 1968, **90**, 319–326.

40 L. Latos-Grazynski, J. Johnson, S. Attar, M. M. Olmstead and A. L. Balch, Reactivity of the verdoheme analogues, 5-oxaporphyrin complexes of cobalt(II) and zinc(II), with nucleophiles: opening of the planar macrocycle by alkoxide addition to form helical complexes, *Inorg. Chem.*, 1998, **37**, 4493–4499.